Comparing the efficiency of scintillating fibres: beta decay electrons vs. muon decay positrons

T. Shiroka, S. Cottrell, P. King

September 22, 2006

Scintillating fibres offer a number of desirable properties for μSR experiments, including nanosecond timing resolution and a low mass presented to the incident particle (down to 50 mg/cm^2 for a 0.5 mm diameter fibre). Fibres may therefore have applications to positron tracking, where it is important to minimise scattering of the incident particle, and high field detectors, where a positron detector may need to be transparent to the incident muons. Despite these excellent properties, scintillating fibres (especially those of low diameter) have suffered from low light output, excluding them from a possible choice as position sensitive and/or high magnetic field detectors in μSR. Indeed, the scarce number of generated photons could be compensated only by the use of high-efficiency, but also very complex, cumbersome and expensive VLPCs[1] detectors. However, recent developments, involving the use of cooled avalanche photodiodes (APD), have shown very promising detection efficiencies ($\sim 100\%$) [1] both in the detection of scintillation light from single fibres, as well as in the readout of fibre bundles [2, 3].

The comparison of these interesting results, obtained with widely available ^{90}Sr beta sources, with those expected in a typical μSR experiment, is crucial for transferring them also to μSR spectroscopy. Some preliminary scintillator tests in a 29 MeV/c muon or positron beam already exist [4], nevertheless a detailed comparison is still missing. Here we present some simple calculation and simulations that clearly show the equivalence of scintillating fibre tests, made with a ^{90}Sr source, with those using muon decay positrons. Apart from a somewhat diminished efficiency ($\varepsilon_{e^+} \sim 0.8\,\varepsilon_{e^-}$), the affirmative answer implies the possibility of extending the already existing literature results also to muon spectroscopy. Since in the energy range of interest ($0.1 \div 50$ MeV) both sources act as MIPs (see Fig. 1), this equivalence is not surprising.

Beta decay electrons vs. muon decay positrons

Strontium-90 (^{90}Sr) is an abundant fission product with a maximum beta-particle kinetic energy, $E_{\max} = 546$ keV and a mean kinetic energy, $\overline{E}_{\beta^-} = 196$ keV. It decays to yttrium-90 (^{90}Y) with a half-life of 29.12 y. The more energetic, short-lived daughter, ^{90}Y ($E_{\max} = 2.28$ MeV and $\overline{E}_{\beta^-} = 933$ keV) decays with a half-life of 64.1 h. Since the daughter has such a short half-life, its emissions are in equilibrium with its parent. The spectra of both these radionuclides are shown in Fig. 1. In case a pure ^{90}Y source is needed, it can be produced by neutron activation of yttrium-89 (^{89}Y) and decays by beta-particle emission with the parameters given above. The equilibrium source ^{90}Sr–^{90}Y has a spectrum which is just the

[1] Visible Light Photon Counter, made by Rockwell International Science Center.

sum of its components' spectra. Both the compound and the simple source are pure β^- emitters. Extensive details about various beta emitters are given in refs. [5, 6, 7].

Electrons from beta decays have a well known characteristic spectrum, which shows a linear behaviour if a *Kurie* plot is used [8]. The analytical spectral shape is given by:

$$N(W) = F(Z, W)(W^2 - 1)^{1/2} W (W_0 - W)^2 a_n(W),$$

where W is the total energy of the electron minus the screening potential, in m_0c^2 units, W_0 is the corresponding value at the maximum electron energy, Z is the atomic number of the daughter nucleus, $F(Z, W)$ is the Fermi function and $a_n(W)$ is a shape factor that depends on the forbiddenness of the transition.
Positrons from muon decay, on the other hand, display a different energy spectrum:

$$N(\varepsilon) = 2(3 - 2\varepsilon)\varepsilon^2,$$

with $\varepsilon = E/E_{\max}$, $E_{\max} = 52.8$ MeV and $\overline{E}_{e^+} = 37$ MeV, shown also in Fig. 1.

Since simulations using the exact energy spectra of beta or positron sources are feasible but complex, the present simulations were restricted to the representative mean energies: $\overline{E}_{1e^-} = 196$ keV and $\overline{E}_{2e^-} = 933$ keV for beta electrons, and $\overline{E}_{e^+} = 37$ MeV for muon decay positrons (all of them are shown by vertical bars in Fig. 1).

Calculation of energy loss in matter

The material we study is a typical plastic scintillator made of polyvinyltoluene (PVT), with $\rho = 1.032$ g/cm^3 and mean excitation energy 64.7 eV. It was chosen because of its higher photon yield (up to 50% brighter) with respect to a polystyrene (PS) based scintillator. As a quick check the electron energy loss for different initial kinetic energies and materials were calculated using the EStar program [9]. Although the preliminary calculations were made for electrons, in the energy range of interest the differences between electrons and positrons, as far as the energy loss is concerned, are minimal (less than 4%)[2].
The total linear stopping power for electrons and positrons is the sum of collisional (ionisation) and radiative losses (bremsstrahlung):

$$\frac{dE}{dx} = \left(\frac{dE}{dx}\right)_c + \left(\frac{dE}{dx}\right)_r.$$

If the particle energy is expressed in MeV, the ratio among the two is given by:

$$\frac{(dE/dx)_r}{(dE/dx)_c} \simeq \frac{EZ}{700}.$$

Since the maximum positron energy in our case is 52.8 MeV and the organic scintillator contains only hydrogen ($Z = 1$) and carbon ($Z = 6$), it is clear that the radiative losses are negligible. As expected, the above ratio approaches 1 only for energies above 107 MeV; for a typical positron energy of 37 MeV it is ~ 0.32 (see Fig. 1). Due to their lower mean kinetic energy (< 1 MeV), the radiative energy loss is even less important in case of beta decay electrons.
In an organic scintillator only the fraction of particle kinetic energy lost to ionisation processes is used to generate optical photons. Although a detailed calculation of the light yield will be

[2]For low kinetic energies, dE/dx for positrons is larger than that for electrons; at about ~ 2 MeV the energy loss is the same; for higher kinetic energies, dE/dx for positron is less than that for electrons [12] (see also Fig. 2).

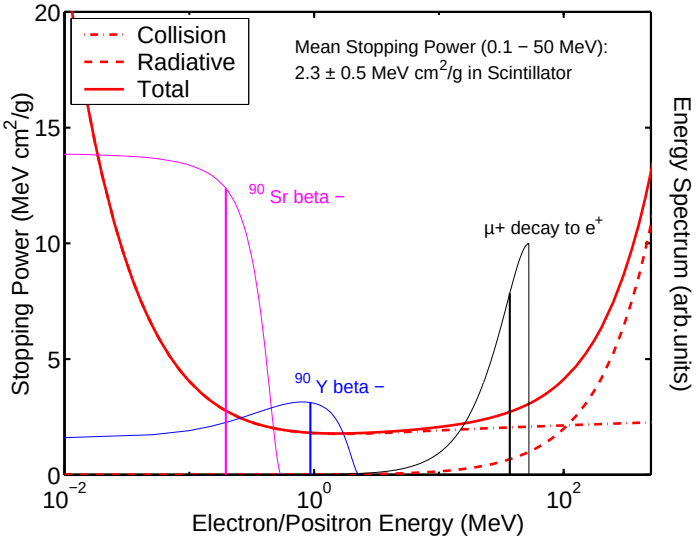

Figure 1: Electron energy loss in a PVT scintillator. The energy spectra of beta decay electrons and muon decay positrons, together with their mean kinetic energies are also shown.

given below, a quick estimate is already possible from Fig. 1. Since the collisional energy loss (dash-dotted line in Fig. 1) is a constantly decreasing function of the particle energy, positrons are expected to display a lower scintillation efficiency. The ionisation rate, however, is almost constant above ~ 1 MeV, hence, the light yield of positrons should be *slightly less* than that of beta electrons. A closer inspection shows a $\sim 20\%$ reduction in efficiency with respect to ^{90}Sr and $\sim 5\%$ reduction with respect to ^{90}Y.

Photon yield for positrons

The previous estimates are useful but not very precise. Moreover, they provide only comparative figures and not the *absolute* photon yield from muon decay positrons. To answer these questions we perform a detailed simulation using the PENELOPE program [10]. Electrons and positrons with the previously mentioned average energies $\overline{E}$ are made to go through a 1 mm thick sheet of PVT scintillating material. Both the specific energy loss (dose) as a function of penetration depth and the total energy loss (dose integral) were calculated and are shown in Fig. 2.

Note that, as anticipated, the difference between electron and positron specific energy loss is negligible. Since the range of 0.35 MeV electrons in a PVT scintillator is $R \simeq 1$ mm (see also Fig. 4), ^{90}Sr beta electrons are mostly stopped in a 1 mm thick scintillator. Indeed, the simulated $\overline{E}_{1e^-} = 0.2$ MeV electrons have a range $R(0.2) = 0.45$ mm and a dose distribution which peaks at 0.2 mm. The only "escaping" electrons are those comprised in the high energy tail ($0.35 \div 0.55$ MeV). On the other hand, the relatively small difference in dose curves at 1 and 37 MeV, shows that the total energy loss is practically energy-independent for $E > 1$ MeV, since particles in this energy range can be considered as minimum ionising particles.

Once the energy loss in matter is known one should be able to find the number of generated photons. In general, the luminescent response of organic scintillators to ionising particles is known to be non-linear [15, 16]. If $d\mathscr{L}/dx$ is the specific luminescence and dE/dx the specific

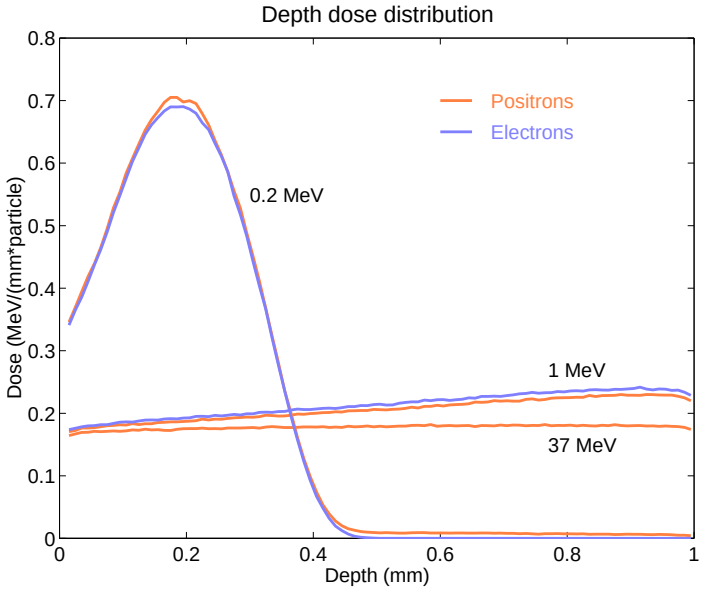

Figure 2: Dose distribution vs. penetration depth in a PVT scintillator for incident particles with different energies. The total dose is given by the area under the curves.

energy loss, the following semi-empirical relation holds:

$$\frac{d\mathscr{L}}{dx} = \mathscr{L}_0 \frac{dE/dx}{1 + k_\mathrm{B} \cdot dE/dx},$$

with $\mathscr{L}_0$ the luminescence at low specific ionisation density and k_B the Birks' constant (to be determined experimentally for each case). This relation reflects both the primary emission by ion recombinations and molecular de-excitation processes. $\mathscr{L}_0 \cdot dE/dx$ represents the number of ionised or excited molecules per unit path length capable of primary emission, whereas $k_\mathrm{B} \cdot dE/dx$ represents the probability of quenching relative to the probability of primary emission. Extensive studies of plastic scintillators have shown that usually only two limiting cases are most often found: $k_\mathrm{B} \cdot dE/dx \ll 1$ applicable to electrons[3], giving $\mathscr{L} = \mathscr{L}_0 E$, and $k_\mathrm{B} \cdot dE/dx \gg 1$, applicable to slow alpha-particles, giving $\mathscr{L} = \mathscr{L}_0/k_B$. The proportionality relation for electrons holds only if all the initial electron kinetic energy is released inside the material, otherwise the luminescence is proportional to the energy deposited during the electron transit.

The light yield is a measure of the capability of the scintillating material to convert radiation energy to fluorescent radiation in or near the visible region. The light yield of a scintillator can be quantified by the average energy loss per scintillator photon [eV/photon]. Often however, the light yield is given relative to the light yield of another scintillator, in most cases NaI or anthracene. The light yield is an important factor which determines the energy resolution at high light levels. At low light levels, as in our case, it determines whether an experiment is feasible or not.

Typical light yield values in common plastic scintillators are 1 photon per 100 eV (10^4 photons per MeV) of deposited energy or, equivalently, 25% of the light output of a NaI(Tl) scintillator or 60% of an anthracene crystal [11, 13]. The simulation data together with the expected number of photons are shown in Table 1. Although 0.2 MeV electrons stop entirely

[3]This relation is valid for relatively fast electrons since their specific energy loss dE/dx is sufficiently small.

Particle	Init. Energy (MeV)	Energy loss (MeV)	Photons	Rel. yield
Electron	0.2	0.194	1937	92%
Electron	1.0	0.211	2109	100%
Positron	37	0.176	1758	83%

Table 1: Energy loss and photon generation for different particles and initial kinetic energies in a 1 mm thick PVT scintillator.

inside the scintillator, the 97% level of energy loss reflects a 3% of backscattered particles. The energy loss from 37 MeV positrons is in very good agreement with other, independent simulations of 560 MeV/c π^+ (which too behave as MIPs), where an energy loss of 110 ± 27 keV was predicted in a 0.66 mm core diameter scintillating fibre [1], to be compared with an extrapolated value of 116 keV from the present simulation.

Scintillating fibers and practical aspects

Although the number of generated photons ($\sim$ 1700) by a 37 MeV positron beam going through a 1 mm thick scintillator might seem large, it is heavily reduced when light transport and attenuation are considered [14]. Indeed, the fraction of generated light which is transported down the optical pipe is denoted the *capture fraction* and is about 6% for a single-clad fibre and 10% for a double-clad fibre [12, 13]. This means that in the best case only 170 photons will be captured. Taking into account a typical attenuation length of 1 m and scintillating fibres 3 m long $(1 - \mathrm{e}^{-3}) \sim 95\%$ of the light will be lost and at the end of the optical fibre will arrive only 5% of the generated photons, i.e. just 9 photons! In a more optimistic case, with one fibre end mirrored and a longer attenuation length (or a shorter fibre), the above figure could double.

These calculations are valid only for positrons crossing a uniform scintillator thickness (square or rectangular profile). In case of cylindrical scintillating fibres with circular cross section, the path length of positrons travelling along a chord, rather than the fibre diameter, would be smaller and therefore the light yield will also diminish. By assuming a uniform distribution of incoming positrons, incident perpendicularly to the fibre axis, the resulting probability distribution functions are:

$$p_c = \frac{2}{\pi R^2} \cdot \sqrt{R^2 - x^2}, \qquad p_s = \frac{1}{2R},$$

where $2R$ is the fibre diameter, or square side and x is the displacement from diameter of the incoming positron path. Both distributions are shown in Fig. 3. In general, the efficiency of a cylindrical fibre will be $\pi/4 \simeq 80\%$ of a square fibre having the same dimensions. If positrons will cross the scintillator at an angle, the path length and the photon yield will increase, but time resolution will deteriorate.

Cylindrical fibres with a reduced diameter (e.g. 0.5 mm instead of 1 mm), provide less light output. For particles incident along the diameter the response will scale linearly. However, in a more realistic case of random incidence, the response will scale *quadratically*, reflecting the reduced fibre cross section. This means that fibres with a diameter of 0.5 mm or less, despite their improved spatial resolution and rather low multiple scattering effects, could scarcely give more than 3 photons at their end, requiring very demanding light detectors, with a quantum efficiency approaching 100% (e.g. cooled APD detectors [1]). Of course, minimising fibre length and optimising other parameters is of paramount importance for bringing this

very poor performance to an acceptable level of S/N ratio. Previous studies have shown that the signal/noise ratio for an MIP would be at least ≥ 4, i.e., the readout of not-too-long scintillating fibers by APDs should be feasible [17].

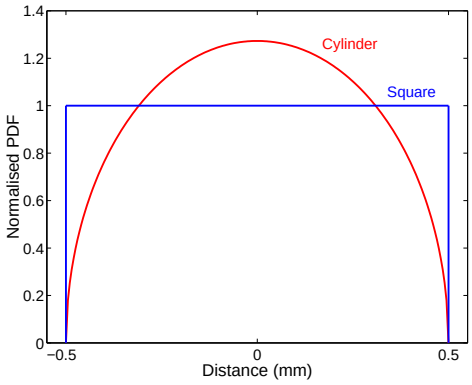

Figure 3: Probability density function (PDF) for energy loss of uniformly distributed positrons incident perpendicularly upon a scintillator with a square or circular cross section.

Positron range and shielding

Positrons are very light particles and lose energy abruptly, therefore their trajectory in matter is far from being linear and one cannot define a range as in case of heavy particles. Nevertheless, the calculation of positron "ranges" in matter is important for an adequate choice of shielding material during tests. Positron ranges in different materials, with high and low Z where calculated and are shown in Fig. 4. As the material density increases the particle range decreases, even though when expressed in g/cm^2 units (not shown), all the curves lie rather close to each other. In preparing an experiment at a muon beam the shielding thickness should be sufficient to stop the highest energy decay positrons ($\sim$ 53 MeV). A 3 cm thick copper or brass shield should be sufficient for this purpose.

As far as the cosmic ray background is concerned, 80% of it is made up of fast muons with a typical intensity of one muon per cm^2 per minute. A sufficiently intense ^{90}Sr or muon beam source would completely overshadow this background effect. For a meaningful comparison the same shielding should be used both in tests with a muon beam and in those with a beta emission source. In general the use of a shielding–collimating configuration as shown in Fig. 5 (see also attachment), together with a coincidence counting with two scintillator paddles, allows measuring the fiber efficiency, defined as: $\varepsilon = n_{\rm ph}/n_{\rm coinc}$, with $n_{\rm ph}$ number of photons measured by the fiber, provided there was a coincidence and $n_{\rm coinc}$ is the total number of coincidences. The S_1 and S_2 scintillator serve as triggers for detecting possible signals from the PMT. If the fiber and S_1 detector are thick, the only particles capable of generating a "good" event would be those having a rather high energy; therefore the energy spectrum would be somehow distorted. The exclusion of low energy particles nevertheless, would not change too much the expected results (see Fig. 1).

The scintillating fiber is placed in a V-guide and excited laterally by a 0.5 mm collimated ^{90}Sr source, or by the muon decay positrons. If needed, the whole test fixture, can be displaced horizontally for checking scintillation light attenuation for different kinds of fibers.

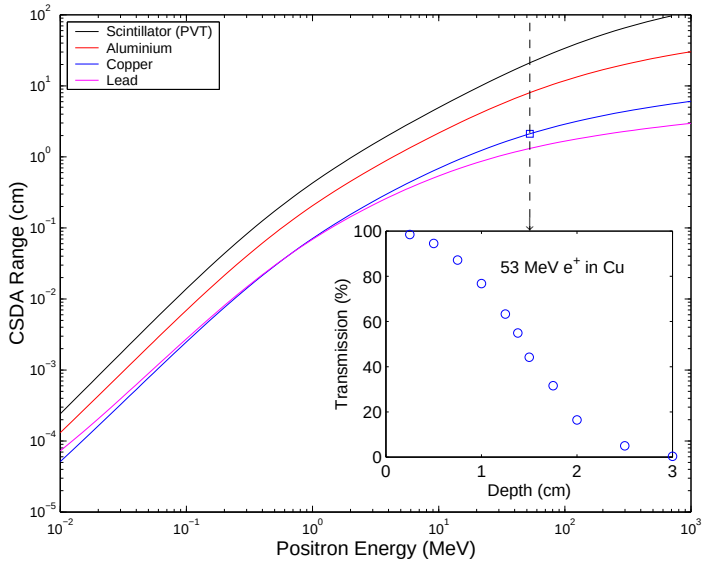

Figure 4: Positron range vs. energy in different materials: PVT Scintillator, Al, Cu and Pb; the dashed line delimits the maximum positron energy (53 MeV). Inset: Simulation of 53 MeV positrons in copper for their range determination ($R = 2.1$ cm).

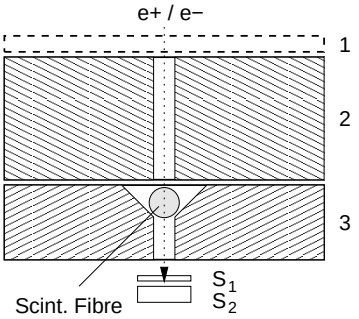

Figure 5: Schematic view (not in scale) of the collimating/shielding configuration. S_1 and S_2 are coincidence scintillators, 1 is a muon stopping target for generating decay positrons. The slit gap for testing 1 mm fibres is 0.5 mm, the shielding thickness of 2 and 3 is ~ 30 mm.

1 Detector choice: PMT vs. APD

The choice of an optical detector for the readout of scintillating fibers is a rather complex issue since it requires the balancing of many disparate factors like: the minimum acceptable signal-to-noise ratio (SNR), the active area, the detector cost, the sensitivity vs. wavelength, the light level to be measured, the time response, etc.

The many excellent properties of the photomultiplier tubes (PMT), most importantly: the superior time resolution, the low-light level and the low-noise performance (arising from an ordinary 10^6 gain), explain their successful use in nuclear and particle physics.

In the past decade though, serious R&D efforts have made possible the use of valid solid-state alternatives, such as the silicon based avalanche photodiodes (APD). Unlike the PMT and other vacuum technologies, APDs are compact and rugged detectors with an extended wavelength response [20]. Differently from their simpler precursor, the PIN diode, the avalanche photodiodes come with an internal gain which easily reaches a factor of 300.

This enables the avalanche photodiode to be used in low light level applications, traditionally dominated by the photomultiplier tube (PMT). Moreover APDs can offer a very high quantum efficiency (up to 90% in the visible, increasing to 100% in the deep UV) and draw much less current than a PMT.

Another recent technological breakthrough, essential to the present work, is the development of multi-element APD devices, allowing the use of APD in position sensing or multi-channel detection applications. Most importantly these APD arrays do not exhibit cross-talk between channels, which is a common limitation with multi-anode PMTs. Another advantage, especially with complex multi-channel applications is the much lower cost with respect to PMTs. This, in addition with the absence of appreciable magnetic field effects makes the APD a very interesting detector for our purposes.

However, despite these very attractive APD properties, at the low light levels available in our case (see previous sections), the large noise-free gain offered by the PMTs could potentially offset their rather low quantum efficiency (QE). The choice becomes even more difficult since, in this regime, the APD behaviour is dominated by the (internal) excess noise factor (due to the avalanche process) and by the (external) amplifier noise.

To effectively confirm the suitability of APDs in a scintillating fiber based position-sensitive detector, accurate preliminary tests are fundamental. For an easy comparison of the two potentially useful detectors their strong and weak features are reported in Tab. 2

PMT	*Advantages*	– High internal gain (10^6) provides excellent S/N ratio – Low light level measurements – Fast recovery time
	Drawbacks	– Poor spatial resolution – Low quantum efficiency and slower rise time – Fragile and bulky – Requires high power supply voltage ($\sim$ 3000 V) – Sensitive to stray magnetic fields
APD	*Advantages*	– High quantum efficiency (almost 100%) – Fast rise time – Highly linear response – Small, rugged and insensitive to magnetic fields – Lower operating voltage ($\sim$ 400 V)
	Drawbacks	– Much lower internal gain ($\sim$ 300), requires cooling – Limited low level signal response – Increased noise (excess noise factor and amplifier)

Table 2: Comparison between PMT and APD main characteristics.

References

[1] T. Okusawa, Y. Sasayama, M. Yamasaki, T. Yoshida, "Readout of a 3 m long scintillating fiber by an avalanche photodiode',' Nucl. Instrum. and Meth. A **459** 440-447 (2001).

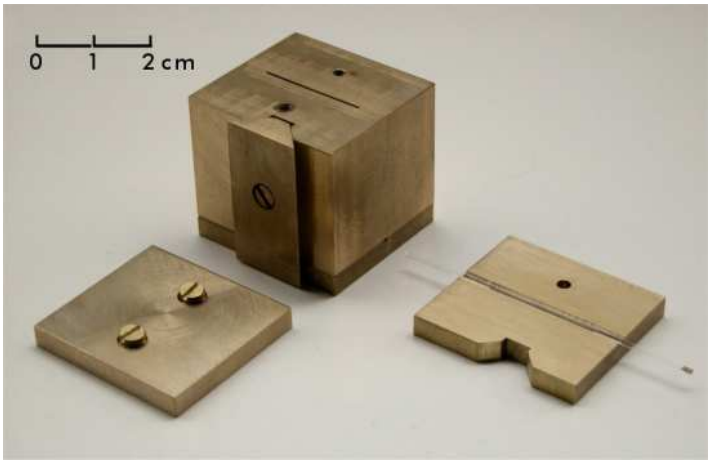

Figure 6: Exploded view of the collimator. The top cover (left) stops the incoming muons, whereas the bottom V-grooved part (right) hosts the scintillating fiber. Both the bottom and central pieces present a 0.5 mm wide slit, which stops most of the incoming particles.

[2] J. R. Macri, A. L. Winterberg, M. Windholm, U. Jagadish, J. Ledoux, M. L. McConnell, S. S. Frank, H. Cutlip, "Readout of Scintillating Plastic Fibers with an APD Array and Prototype ASIC", IEEE Trans. Nucl. Sci., **50**, 928-935 (2003).

[3] T. Yoshida, T. Sora, "A prototype avalanche photodiode array for scintillating-fiber tracking detectors" Nucl. Instrum. and Meth. A **534** 397-402 (2004).

[4] V. V. Zhuk, R. Scheuermann, A. V. Stoykov, "Light Collection Efficiency from Thin Plastic Scintillators", PSI Technical Report TM-35-05-01.

[5] W. G. Cross, H. Ing, and N. Freedman, "A short atlas of beta-ray spectra", Phys. Med. Biol., **28** (11), 1251-1260 (1983).

[6] R. S. Caswell, P. M. DeLuca, S. M. Seltzer, and A. Wambersie, "Sources and their application in brachyterapy", J. ICRU, **4** (2), 21-28, (2004), Report 72, OUP.

[7] <http://atom.kaeri.re.kr/ton/main.shtml>, Jan. 2006.

[8] F. N. D. Kurie, J. R. Richardson, and H. C. Paxton, "The Radiations Emitted from Artificially Produced Radioactive Substances. I. The Upper Limits and Shapes of the β-Ray Spectra from Several Elements", Phys. Rev., **49** (5), 368-381, (1936).

[9] <http://physics.nist.gov/PhysRefData/Star/Text/ESTAR.html>, Jan. 2006.

[10] J. Sempau, E. Acosta, J. Baro, J. M. Fernandez-Varea and F. Salvat, "An algorithm for Monte Carlo simulation of coupled electron-photon transport", Nucl. Instrum. and Meth. B **132** 377-390 (1997).

[11] Marketech International, Inc., Port Townsend, WA, <www.mkt-intl.com>, Jan. 2006.

[12] N. Tsoulfanidis, *Measurement and Detection of Radiation*, 2nd ed., Taylor and Francis, London, 1995.

[13] G. F. Knoll, *Radiation Detection and Measurement*, 3rd ed., John Wiley & Sons, Hoboken, NJ, 2000.

[14] K. F. Johnson, "Organic scintillators", in S. Eidelman, *et al.*, Physics Letters B **592**, 1 (2004). See also PDG web page at <http://pdg.lbl.gov >.

[15] J. B. Birks, *The Theory and Practice of Scintillation Counting*, Pergamon Press, Oxford, 1964.

[16] H. C. Evans, and E. H. Bellamy, "The Response of Plastic Scintillators to Protons", Proc. Phys. Soc. **74** 483-485 (1959).

[17] E. Lorenz, B. Pichler, W. Pimpl, S. Ziegler, R. Mirzoyan, "Test of a scintillating fiber readout with avalanche photodiodes", Nucl. Instrum. and Meth. A **504** 154-160 (2003).

[18] H. Leutz, "Scintillating fibers", Nucl. Instrum. and Meth. A **364** 422-448 (1995).

[19] R. Ruchti, "The use of scintillating fibers for charged-particle tracking", Annu. Rev. Nucl. Part. Sci., 46 (1996) 281.

[20] Advanced Photonix, Inc, Photodiodes and Avalanche Photodiodes, <http://www.-advancedphotonix.com>, Jan. 2006.